Appl. Phys. B 87, 79–84 (2007)
DOI: 10.1007/s00340-006-2488-3

Applied Physics B
Lasers and Optics

J.A. FÜLÖP[1,2,✉]
ZS. MAJOR[1]
B. HORVÁTH[1]
F. TAVELLA[1]
A. BALTUŠKA[1]
F. KRAUSZ[1,2]

Shaping of picosecond pulses for pumping optical parametric amplification

[1] Max-Planck-Institut für Quantenoptik, Hans-Kopfermann-Str. 1, 85748 Garching, Germany
[2] Department für Physik, Ludwig-Maximilians-Universität München, Am Coulombwall 1, 85748 Garching, Germany

Received: 29 September 2006
Published online: 18 November 2006 •

ABSTRACT The use of temporally shaped pump pulses for optical parametric chirped-pulse amplification can increase the efficiency and suppress possible spectral distortions in this process. With this goal in mind a novel method for shaping narrowband picosecond pulses has been developed. The method is based on the pulse stacking principle, where replicas of the incoming pulse are created in a specially designed four-beam interferometer. The replicas are recombined with appropriate relative delays. The interferometer design allows for a unique flexibility in varying the pulse shape, since all relevant degrees of freedom, such as relative intensities and delays between the pulse replicas are independently adjustable. Here we describe the design of our device in detail and report on the experimental demonstration of its pulse-shaping capabilities.

PACS 42.65.Yj; 42.65.Re; 42.81.Gs

1 Introduction

In recent years the technique of optical parametric amplification (OPA) has opened up a new path towards generating few-cycle laser pulses with unprecedented peak powers [1–9]. Such pulses are crucial for the investigation of laser-driven strong-field phenomena [10], having become an accessible field of research with the advent of suitable laser systems.

In the OPA process amplification takes place in a nonlinear optical crystal, where phase-matching in a non-collinear geometry allows for extremely large amplification bandwidths [1], and thereby enables the amplification of broadband seed pulses using relatively narrowband pump pulses delivered by conventional laser amplification technology. In order to reach the highest possible peak intensities, OPA is usually combined with chirped-pulse amplification, called optical parametric chirped-pulse amplification (OPCPA), a scheme first proposed by Dubietis et al. [11].

In the OPA process the resulting gain sensitively depends on the pump intensity [12, 13] and hence on the temporal and spatial shape of the pump pulse. In most cases a pump pulse with a Gaussian temporal profile is used. If a uniform gain is to be achieved, the pump pulse has to be significantly longer than the seed in order to keep the pump intensity approximately constant during amplification. In this case, however, a large fraction of the pump energy is discarded (cf. Fig. 1a), thereby lowering the overall efficiency of the OPA process. However, if the seed and pump pulses are of comparable duration, generally the gain along the seed pulse will be non-uniform, resulting in a distortion of the amplified pulse (cf. Fig. 1b). For a strongly chirped seed pulse this effect can possibly lead to a significant decrease of the spectral bandwidth. However, these problems could possibly be avoided by controlling the temporal shape of the pump pulse, as qualitatively shown in Fig. 1c. A pump pulse with a rectangular temporal profile and a duration comparable to that of the seed pulse would provide a uniform gain of all spectral components, thereby avoiding spectral distortion and increasing the pump-to-signal conversion efficiency. If the seed profile shows a more complicated structure, as is often the case in very broadband oscillators, a shapable pump pulse would allow to compensate for such structure and to obtain of an amplified pulse as desired. The advantage of using pump pulses, shaped both in space and time, on the OPA conversion efficiency has been previously demonstrated by Waxer et al. [14] in the case of $\sim$ 1-ns pulses and a relatively narrowband seed signal.

In order to quantitatively assess how the efficiency and uniformity of the OPA process benefit from temporally shaped pump pulses, we performed calculations with three different pump-pulse temporal profiles (Fig. 1d), namely (i) flat-top profile of 50 ps duration, i.e. constant pump intensity; (ii) Gaussian profile; (iii) a temporally shaped pulse. This last case corresponds to our experimental situation as described in Sects. 2 and 3, closely approaching an ideal square-shaped pulse. In all cases the seed pulse was a rectangular 50 ps pulse representing the strongly stretched output of an ultrabroadband oscillator with a spectrum covering the gain bandwidth of the OPA crystal. Details of the calculations are given below[1]. The resulting gain curves alongside the respective pump-pulse profiles are shown in Fig. 1d and

✉ Fax: +49-89-32905-200, E-mail: jozsef.fulop@mpq.mpg.de

[1] In order to obtain the OPA gain the coupled wave equations (see e.g. [12]) were solved numerically by neglecting group-velocity dispersion effects, which is justified by the strong initial chirp of the seed pulses. For a simulation as close as possible to a realistic experimental setup we assumed a system consisting of two OPA stages. The first stage was operated in the small-signal gain regime, while in the second stage

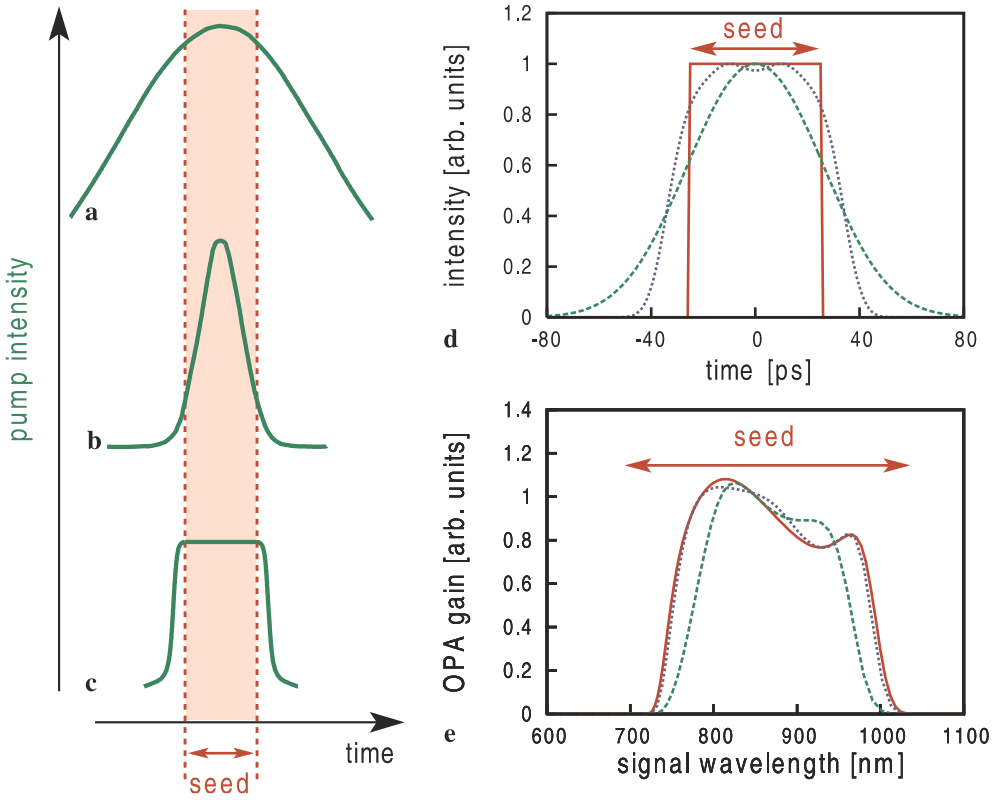

FIGURE 1 *Left*: (**a**)–(**c**) OPCPA with differently shaped pump pulses. The time window of the seed pulse is indicated by the shading. *Right*: Results of OPCPA gain calculations. The different pump-pulse shapes are shown in (**d**): (i) flat top (*solid/red line*), (ii) Gaussian (*dashed/green line*), and (iii) shaped pulse (*dotted/blue* line). (**e**) shows the corresponding gain *curves* together with the spectral range of the seed pulse

Pulse shape	τ_p [ps]	E_p [mJ]	E_s [mJ]	η [%]
(i) flat top	50	1.06	0.352	33.2
(ii) Gaussian	60	1.34	0.280	20.9
(iii) shaped pulse	65	1.34	0.344	25.7
(iv) Gaussian	138	3.10	0.338	10.9

TABLE 1 Comparison of OPCPA performance with pump pulses of different temporal shapes. τ_p is the pump-pulse duration (intensity FWHM), E_p and E_s are the energies of the pump pulse and the amplified signal, respectively, and η is the pump-to-signal conversion efficiency[2]. The gain curves corresponding to cases (i)–(iii) are shown in Fig. 1

e, the corresponding conversion efficiencies are summarized in Table 1. As expected, the best performance both in terms of amplification bandwidth as well as in conversion efficiency is achieved with the rectangular pump pulses. Here the gain bandwidth is only limited by the phase-matching bandwidth of the crystal. In order to essentially preserve this bandwidth with the shaped pump pulses of type (iii), the pulse duration has to be slightly longer, namely 65 ps. This in turn leads to a drop in the pump-to-signal conversion efficiency. Using a Gaussian pump pulse (ii) of the same energy further decreases the efficiency and, in addition, the gain bandwidth is dramatically reduced, due to the small gain at the wings of the pulse. The full gain bandwidth of the crystal can only be restored by increasing the duration of the Gaussian pump pulse by more than a factor of two (i.e. 138 ps). This, of course, requires a lot more pump energy and therefore gives a conversion efficiency which is 2.4 times smaller than with the shaped pulse (iii).

Having seen the advantages of temporally shaped pump pulses predicted by simulations we now turn to the question of how to carry out such shaping on characteristic time scales of OPCPA systems. In typical ultrabroadband OPCPA systems the duration of pump pulses, obtained from a Nd:YAG laser, are usually of the order of 100 ps [7–9]. This time scale lies below the limits of fast (opto)electronics, which therefore cannot be used for shaping such pulses. However, the corresponding bandwidth, typically a fraction of a nanometer, is too narrow to allow for conventional shaping methods based on spectral filtering, used in the femtosecond regime.

The question of a passive pulse-shaping device in the picosecond regime has been the subject of a number of earlier studies [15–21], mostly motivated by applications in the field of laser-induced fusion. While some of these methods spatially shape the pulses and subsequently transform the obtained structure into the temporal domain [16–18], most approaches are based on the principle of pulse stacking [19–21]. Here a number of replicas of an input pulse are created, then delayed with respect to each other, and finally recombined to

depletion of the pump occurred. The crystal thickness was 4.4 mm in both stages, the pump energies and the beam diameters were equal, too. The pump wavelength was 532 nm. For maximum amplification bandwidth non-collinear phase matching was assumed in a β-barium-borate (BBO) crystal for the 850 nm seed central wavelength. The spatial profiles of both the seed and the pump beams were Gaussian with 0.7 mm diameter (at $1/e^2$ of the maximum intensity). The shaped pump pulse (iii) was made up of four 19 ps pulses with a relative delay of 20.6 ps between them, and subsequently frequency doubled with 50% conversion efficiency. For a good comparison between the differently shaped pump pulses the peak intensity was 11 GW/cm^2 in all cases.

[2] The values for E_p, E_s and η given in Table 1 correspond to the second OPA stage. The conversion efficiency in the first stage was very low due to operation in the small-signal gain regime.

give an output pulse of the desired shape. The resulting pulse shape is extremely sensitive to the relative delays and phases of the replicas on an interferometric scale, thus the realization of this simple scheme is not straightforward. Several setups have been designed for this purpose, allowing a composition of the output pulse from up to 20 individual pulses [19]. It is clear that the more replicas are used, the finer the final shape of the pulse can be adjusted. However, in previous designs it was not possible to vary the degrees of freedom which determine the resulting pulse shape independently, thereby limiting the possible output shapes in spite of the large number of pulse replicas. Therefore, we present a novel setup for the shaping of picosecond time-scale pulses based on the pulse-stacking principle, using only four replicas of the input pulse, but allowing for individual adjustment of all possible degrees of freedom. This enables the synthesis of any pulse shape allowed by the pulse-stacking principle without any additional constraints.

In the following section we first give details of our apparatus, then we demonstrate its operation by presenting almost arbitrarily shaped pulses, and finally we show how pulse shapes can be chosen to "precompensate", for instance, for the non-uniformity of a laser amplifier. We show that in this way we can obtain laser pulses with shapes, which we believe would be ideal for pumping OPCPA stages without distorting the seed pulse or discarding a large portion of the pump energy.

2 Experimental setup

The design of the pulse-stacking interferometer is shown schematically in Fig. 2. The incoming beam is split into four replicas using two pairs of birefringent prisms made of YVO_4 crystals. The orientation of the prisms relative to the polarization of the incoming beam is such that the beam entering the first prism is split into an ordinary and an extraordinary beam. The propagation directions of these two beams are made parallel by the second prism of the first pair, which is placed at some distance. This distance determines the spatial separation of the beam replicas. The second prism pair is rotated by 90° with respect to the first, and, working on the same principle, splits the two separated parts of the beam into two parts each, creating a total of four replicas. A $\lambda/2$ waveplate is placed in front of both the first and the second prism pairs, allowing to rotate of the polarization direction so that the resulting replicas are of equal intensities. In our design the location of the four beam replicas formed the corners of a square.

The four parts of the input beam are retroreflected by an end mirror consisting of four square segments, each mounted separately. The optical path of each of the pulse replicas can be chosen independently by changing the positions of these segments along the beam direction. By delaying the pulses with respect to each other in this way and recombining the reflections off the end mirrors in the backward pass (which coincides with the path of the input pulse), we obtain the desired shaped pulse, consisting of the superimposed pulse replicas. Separating the input pulses from the output pulses is made possible in the following way. A thin-film polarizer is placed in front of the first prism pair. The $\lambda/2$ waveplate in front of the prisms and the orientation of the optical axis of the prism pairs ensure that the polarization of the output beam is perpendicular to that of the input beam, and therefore the returning shaped pulse will be coupled out of the shaping device by the thin-film polarizer.

Four $\lambda/4$ waveplates are inserted into the beam path, one into the path of each pulse replica, before the reflection off the end mirror. Each pulse replica double passes this waveplate, therefore, by choosing their rotation individually, the polarization direction and hence the relative amplitude of each pulse replica can be adjusted independently.

The described degrees of freedom of our design allows us to synthesize pulses of almost arbitrary temporal shapes. In the second part of this section the properties of the above described design and its output pulse shapes are discussed.

The resulting pulse shapes in a pulse-stacking interferometer depend, in general, very sensitively on the relative phases between the pulse replicas, i.e. on the delays of the replicas on the interferometric scale. For long-term stability it is therefore very important to choose optomechanical components for the pulse shaper which are stable on such a length scale. After setting the positions of the mounts of the end mirror segments, the adjustments on the interferometric scale can be carried out by slightly changing the tilt angle on each segment. It turned out, however, that two of the three relative phases between the four replicas can be set in a more convenient way, namely by moving the second prism of each pair into and out of the beam, thereby slightly changing the optical path.

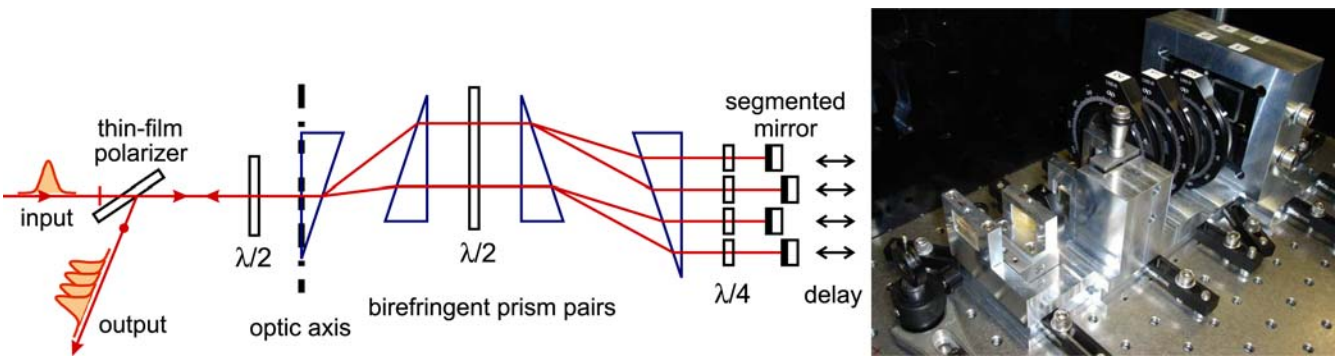

FIGURE 2 *Left*: Schematic setup of the pulse-stacking interferometer. The second pair of prisms is rotated by 90° about the beam direction. *Right*: Photograph of our pulse-stacking setup

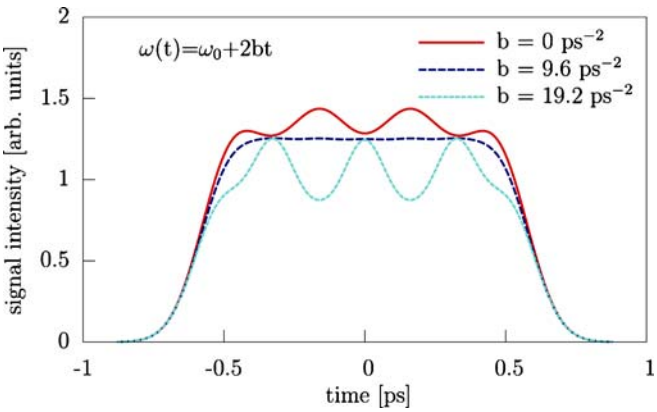

FIGURE 3 Effect of input pulse chirp on the shape of the output pulse. The input pulse duration was 250 fs, the delay between pulse replicas was 1.3 × 250 fs. The chirp values are of the order of that introduced by our pulse shaping device

Since the long-term stability on the interferometric scale constitutes one of the main questions to be solved when designing an interferometric pulse stacker, we have applied the following design features: (i) we minimized the number of moving parts in the device, making adjustments somewhat more difficult, but clearly improving the stability; (ii) a solid aluminium block formed the base of the entire pulse shaper allowing for a very compact design; (iii) a perspex housing minimized environmental influences such as air turbulence. We found that even though such a pulse-shaper device is expected to be extremely sensitive to temperature fluctuations, in our case, in a normal laboratory environment, an active thermal stabilization was not necessary.

The throughput of our pulse-shaping device depends on the actual pulse shape, but varies typically in the range between 20% and 25%. The losses are mainly due to the generation of additional beams in the backward pass through the prism pairs. Since the pulse shaping can be done before boosting the pulse energy (in a conventional laser amplifier) to high enough values required for OPA pumping, these losses can usually be easily tolerated.

The limit of our pulse-stacking concept in terms of pulse duration is set by the material dispersion of the optical components. The chirp of the pulse replicas influences the shape of the stacked output pulse, as can be seen from our calculation shown in Fig. 3. It is interesting to note that a small amount of chirp leads to an even better flat-top output pulse by smoothing ripples present in the unchirped case. However, further increasing the chirp results in growing intensity modulations and therefore a strongly distorted pulse shape. According to our calculations, input pulses as short as ∼200 fs can be used with our setup without causing significant distortions. It should also be noted that the concept of our pulse stacker is not limited to four pulse replicas, and could in principle be extended to any number. With a larger number of replicas, details of the shaped pulse could be determined on a finer scale. However, increasing the number of beam splitters and end-mirror segments would make the mechanical design much more complicated.

In the following section we will demonstrate and discuss the pulse-shaping capabilities of our design by presenting our experimental investigations.

3 Results and discussion

For testing the capabilities of our pulse-shaping device we used input pulses from a passively mode-locked Nd:vanadate oscillator (High Q Laser) with a wavelength of 1064 nm, pulse energy of 6 nJ, and a duration of 19 ps. The four pulse replicas were delayed with respect to each other by ∼ 1.3 times the width of a single pulse, i.e. ∼ 25 ps. This re-

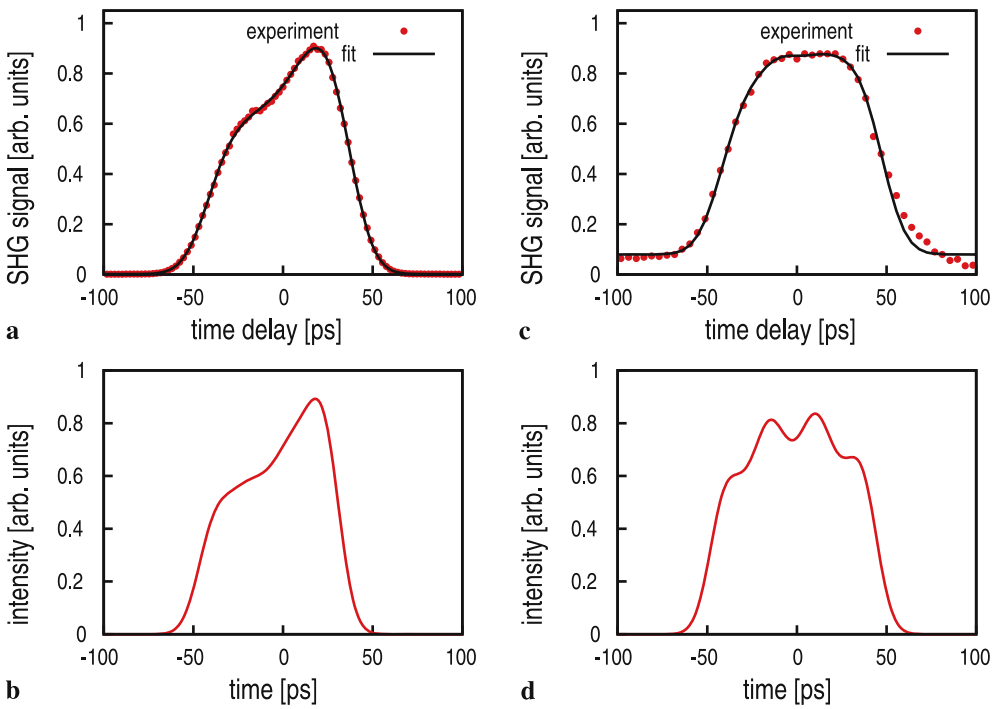

FIGURE 4 Cross correlation of shaped pulses (**a**) prior to and (**c**) after amplification. Figures (**b**) and (**d**) show the corresponding pulse shapes inferred from the fitting

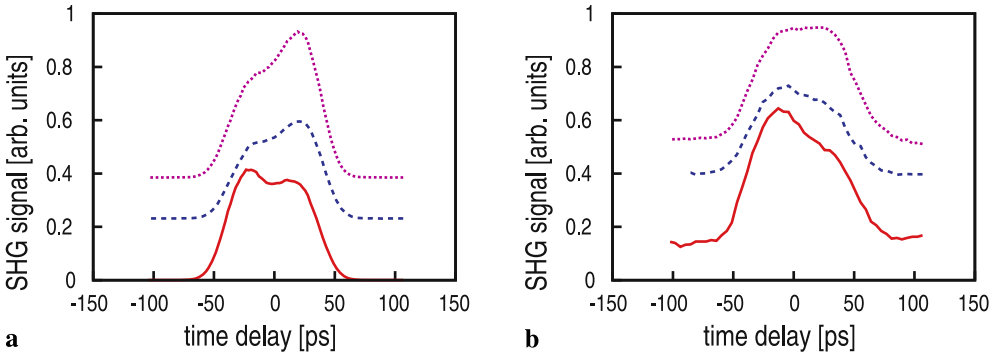

FIGURE 5 Cross correlation of shaped pulses with different top slopes (**a**) prior to and (**b**) after amplification. Colors indicate the corresponding measurements

sulted in a shaped pulse with an approximate duration of 80 ps and a pulse energy of about 1 nJ. The energy losses are mainly due to the relatively low throughput of the pulse stacker.

In order to assess the output pulse shape we performed cross-correlation measurements, using part of the unshaped input pulse as a reference pulse. Although such a relatively long reference pulse limits the scale on which temporal structure can be resolved by cross correlation, it was still sufficient for verifying that a large range of different pulse shapes can be created with our interferometric pulse stacker.

As mentioned in Sect. 1, in most systems the shaped pump pulses would have to be amplified in a conventional laser amplifier prior to their application as pump pulses for an OPCPA stage. Therefore, we also investigated the behaviour of the shaped pulses when passing through a two-stage Nd:YAG amplifier (EKSPLA). The first stage was a regenerative amplifier (regen), followed by a double-pass power amplifier. The relatively low seed energy for the regen on the order of about 10 pJ was due to additional losses (in some low-throughput optics) between the pulse-shaper output and the amplifier input, but it was still sufficient for achieving an overall amplification gain of 10^7–10^8 after ~ 35 round trips. The regen output energy was ~ 2 mJ. These pulses were then amplified to ~ 100 mJ in the power amplifier.

Our results and findings are summarized in Figs. 4 and 5. Firstly, we were able to create a large range of different pulse shapes using our pulse stacker with four pulses. The cross correlation of one of these shapes is shown in Fig. 4a. Using a fitting procedure[3] we extracted the "real" pulse shape, i.e. by eliminating the effect of convolution with the reference pulse. The "reconstructed" pulse shape is shown in Fig. 4b. Secondly, we demonstrated that it is possible to amplify our shaped pulses. Figure 4c and d show the cross correlation and the "deconvoluted" pulse shape from the fit for such an amplified pulse, respectively. It is clear that in both cases, i.e. before and after amplification, the cross-correlation trace resembles the shaped pulses in good detail, and can therefore be used to characterize our pulse-shaping device.

As discussed in Sect. 1 the best results in OPA are obtained for pump pulses with temporal profiles as close as possible to a flat-top shape. Therefore, our aim is to create a temporal pulse profile which after amplification has a flat top. In the conventional laser amplification process the temporal shape of a pulse is distorted in the following ways. Firstly, owing to gain depletion the rising edge of the pulse will experience higher amplification than the trailing edge which reaches the laser medium at a later time. Thus, a flat-top-shaped amplified pulse requires an input pulse which has a sloping top, similar to that shown in Fig. 4c, but in the opposite direction. The capability of our pulse stacker for such precompensation of the distortions introduced by the amplifier can be seen in Fig. 5a and b. Here we have measured the cross correlation both before and after amplification for differently shaped pulses. We can clearly see that the slope of the pulse tops is altered in the laser amplifier and that it is possible to choose a set of delays and relative amplitudes in our pulse stacker that allows to create of a nearly flat-top temporal profile. Furthermore, in Fig. 5 we can also see that the rise and fall times of the amplified pulses appear to have slightly increased in comparison with the pulses prior to amplification. The reason for this lies in the so-called gain narrowing of the amplifying medium. For the high gain obtained in our case the amplification bandwidth of the Nd:YAG does not support 19 ps pulses. This pulse distortion effect could, in principle, be overcome by choosing a different amplifier medium with broader gain bandwidth.

It should be noted that possible ripples on the top of the stacked pulses may be intolerable in OPCPA stages where the gain is high and the pump-to-signal conversion efficiency is low. In this case, the amplified seed spectrum very sensitively depends on intensity variations of the pump pulse. However, shaped pump pulses are important in OPCPA stages with high conversion efficiency and small gain, e.g. in the last stage of a multi-stage setup. Here the ripples have less influence on the signal pulse.

In conclusion, we have demonstrated the shaping and amplification of picosecond pulses to the 100 mJ level using a novel pulse-shaping interferometer based on the pulse-stacking principle. Our shaper design allows for the synthesis of any pulse shapes possible with pulse stacking. Such pulses can be used as pump pulses in OPCPA, allowing for optimization of this technique.

[3] We performed a least-squares fit of a model pulse to the measured cross correlation. For the model pulse we assumed that it was made up of four Gaussian pulses with 19 ps duration, variable time delays and amplitudes. For the case of amplified pulses we used the Frantz–Nodvik model [22] for calculating the effect of laser amplification. While this theory accounts for the effect of gain depletion, it cannot describe the gain narrowing experienced at high amplification factors.

ACKNOWLEDGEMENTS The authors gratefully acknowledge the help of N. Ishii. Financial support from the XTRA network (contract No.: MRTN-CT-2003-505138, Zs.M. and B.H.) and the Marie-Curie Individual Fellowship No.: MEIF-CT-2005-024150 (Zs.M.) is also acknowledged. This work was also supported by funds from the Participating Organisations of EURYI (see www.esf.org/euryi).

REFERENCES

1 G.M. Gale, M. Cavallari, T.J. Driscoll, F. Hache, Opt. Lett. **20**, 1562 (1995)
2 T. Wilhelm, J. Piel, E. Riedle, Opt. Lett. **22**, 1494 (1997)
3 I.N. Ross, P. Matousek, M. Towrie, A.J. Langley, J.L. Collier, Opt. Commun. **144**, 125 (1997)
4 G. Cerullo, M. Nisoli, S. Stagira, S. De Silvestri, Opt. Lett. **23**, 1283 (1998)
5 A. Shirakawa, I. Sakane, M. Takasaka, T. Kobayashi, Appl. Phys. Lett. **74**, 2268 (1999)
6 A. Baltuska, T. Kobayashi, F.X. Kärtner (Ed.), Top. Appl. Phys. **95**, 179 (2004)
7 N. Ishii, L. Turi, V.S. Yakovlev, T. Fuji, F. Krausz, A. Baltuska, R. Butkus, G. Veitas, V. Smilgevicius, R. Danielius, A. Piskarskas, Opt. Lett. **30**, 567 (2005)
8 S. Witte, R.T. Zinkstok, W. Hogervorst, K.S.E. Eikema, Opt. Express **13**, 4903 (2005)
9 S. Witte, R.T. Zinkstok, A.L. Wolf, W. Hogervorst, W. Ubachs, K.S.E. Eikema, Opt. Express **14**, 8168 (2006)
10 T. Brabec, F. Krausz, Rev. Mod. Phys. **72**, 545 (2000)
11 A. Dubietis, G. Jonusauskas, A. Piskarskas, Opt. Commun. **88**, 437 (1992)
12 G. Cerullo, S. De Silvestri, Rev. Sci. Instrum. **74**, 1 (2003)
13 I.N. Ross, P. Matousek, G.H.C. New, K. Osvay, J. Opt. Soc. Am. B **19**, 2945 (2002)
14 L.J. Waxer, V. Bagnoud, I.A. Begishev, M.J. Guardalben, J. Puth, J.D. Zuegel, Opt. Lett. **28**, 1245 (2003)
15 J. Desbois, F. Gires, P. Tournois, IEEE J. Quantum Electron. **QE-9**, 213 (1973)
16 P. Emplit, J.-P. Hamaide, F. Reynaud, Opt. Lett. **17**, 1358 (1992)
17 B. Colombeau, M. Vampouille, C. Froehly, Opt. Commun. **19**, 201 (1976)
18 C. Froehly, B. Colombeau, M. Vampouille, in: *Progress in Optics XX.*, ed. by E. Wolf (North-Holland, Amsterdam, 1976), p. 65
19 W.E. Martin, D. Milam, Appl. Opt. **15**, 3054 (1976)
20 C.E. Thomas, L.D. Siebert, Appl. Opt. **15**, 462 (1976)
21 C.W. Siders, J.L.W. Siders, A.J. Taylor, S.G. Park, A.M. Weiner, Appl. Opt. **37**, 5302 (1998)
22 L.M. Frantz, J.S. Nodvik, J. Appl. Phys. **34**, 2346 (1963)